

Effects of ROCK Inhibitors on Apoptosis of Corneal Endothelial Cells in CMV-Positive Posner–Schlossman Syndrome Patients

Nozomi Igarashi, Megumi Honjo, Toshikatsu Kaburaki, and Makoto Aihara

Department of Ophthalmology, Graduate School of Medicine, The University of Tokyo, Tokyo, Japan

Correspondence: Makoto Aihara, Department of Ophthalmology, University of Tokyo School of Medicine, 7-3-1 Hongo Bunkyo-ku, Tokyo 113-8655, Japan; aihara-ky@umin.net.

Received: February 3, 2020

Accepted: May 31, 2020

Published: August 4, 2020

Citation: Igarashi N, Honjo M, Kaburaki T, Aihara M. Effects of ROCK inhibitors on apoptosis of corneal endothelial cells in CMV-positive Posner–Schlossman syndrome patients. *Invest Ophthalmol Vis Sci.* 2020;61(10):5. <https://doi.org/10.1167/iovs.61.10.5>

PURPOSE. To examine the role of aqueous tumor necrosis factor α (TNF- α)–RhoA–Rho kinase (ROCK) signaling in cytomegalovirus (CMV)-induced apoptosis and the barrier function of cultured human corneal endothelial cells (hCECs) in CMV-positive Posner–Schlossman syndrome (CMV+/PSS) patients.

METHODS. Aqueous levels of TNF- α , IL-8, IL-10, and several other cytokines in 19 CMV+/PSS patients and 20 healthy control subjects were quantitated using a multiplex assay. The expression of active RhoA in hCECs post-CMV infection was determined using western blotting (WB). The expression levels of TNF- α and nuclear factor kappa B (NF- κ B) in CMV-infected hCECs were examined by immunocytochemistry (ICC) and WB with and without ROCK inhibitors. The apoptotic rate and barrier integrity in CMV-infected hCECs were also examined.

RESULTS. The expression levels of TNF- α , monocyte chemoattractant protein-1 (MCP-1), IL-8, and IL-10 were upregulated in the aqueous humor of CMV+/PSS patients, and among these upregulated cytokines aqueous TNF- α was negatively correlated with the number of corneal endothelial cells. In CMV-infected hCECs, upregulation of TNF- α and NF- κ B was determined by WB and ICC. In hCECs, CMV infection induced apoptosis and significantly impaired cell–cell contacts, effects that were attenuated by treatment with a ROCK inhibitor.

CONCLUSIONS. Aqueous TNF- α was upregulated in CMV+/PSS patients, which may have triggered corneal endothelial cell loss. Modulation of TNF- α , including its downstream Rho–ROCK signaling, could serve as a novel treatment modality for corneal endothelial cell loss in CMV+/PSS patients.

Keywords: human corneal endothelial cells, tumor necrosis factor alpha, cytomegalovirus, Posner–Schlossman syndrome, ROCK inhibitor

Posner–Schlossman syndrome (PSS) is characterized by unilateral anterior uveitis (AU), causing recurrent episodes of elevated intraocular pressure (IOP),¹ especially in males. Many previous studies have reported the involvement of cytomegalovirus (CMV) in the pathogenesis of PSS.^{2–8} For example, Chee et al.² reported that 52.2% of suspected PSS patients were CMV-positive for aqueous humor (AH). Regarding the decrease of corneal endothelial cells in CMV-positive AU patients, several cytokines have been reported to be upregulated in the AH of these patients, but the mechanism of endothelial cell loss and the relationship between these upregulated cytokines are poorly understood; there is no effective treatment for preserving corneal endothelial cells.

TNF- α is one of the T-helper 1 (Th1) immune mediators that is reportedly upregulated in various types of uveitis.⁹ Especially in PSS eyes, it has been previously reported that the levels of aqueous TNF- α were significantly increased compared to control eyes (i.e., eyes without any complications), which could be related to the induction of inflammation in PSS patients.^{10–13} Numerous studies have reported that TNF- α plays a role in corneal

endothelial cell loss, because it induces apoptosis, cellular barrier dysfunction, and prolonged immune responses via induction of the expression of higher cellular adhesion molecules.^{11,14–24} It has been shown that, upon infection, CMV replicates in corneal endothelial cells in vitro,²⁵ and endothelial cells infected with CMV rapidly induce apoptosis to inhibit viral growth.²⁶ Rho–Rho kinase (ROCK) signaling occurs downstream in TNF- α -mediated pathophysiological disorders, resulting in endothelial damage, apoptosis, and/or higher cellular permeability^{27–29}; however, few studies have focused on the involvement of TNF- α –Rho–ROCK signaling in damage to corneal endothelial cells. Therefore, in the present study, we sought to determine if aqueous TNF- α is involved in the pathophysiology of corneal endothelial cell loss in CMV-positive PSS patients. We then investigated whether CMV-induced corneal endothelial cell apoptosis could be attenuated by ROCK inhibitors. Our results showed that the TNF- α -induced activation of Rho–ROCK signaling was a crucial event not only in the loss of barrier integrity and disruption of the cytoskeleton but also in the loss of corneal endothelial cells.

PATIENTS AND METHODS

Patients and AH Samples

AH samples were obtained March 2014 to July 2018 at the University of Tokyo Hospital from patients who underwent cataract surgery and were confirmed negative for CMV DNA in the aqueous humor by PCR testing, as well as from patients with clinical signs of CMV AU who underwent PCR testing and were confirmed positive for CMV DNA in the aqueous humor. This prospective observational study was approved by the Institutional Review Board of the University of Tokyo and was registered with the University Hospital Medical Information Network Clinical Trials Registry of Japan (ID: UMIN000027137). All procedures conformed to the tenets of the Declaration of Helsinki, and written informed consent was obtained from all patients.

The inflammation was analyzed according to the criteria of the Standardization of Uveitis Nomenclature (SUN) working group, including in terms of the anatomical location, onset, duration, course, and activity.³⁰ The diagnostic criteria for PSS were as follows: recurrent elevated IOP (>21 mm Hg) and mild (SUN grade of 1) intermittent anterior chamber inflammation with fine-to-medium-sized keratic precipitates and unilateral eye involvement. Exclusion criteria included the presence of other types of ocular diseases; possible systemic, genetic, or infectious origin of the inflammation; or a previous history of intraocular surgery other than small-incision cataract surgery without complications. All patients were negative for tuberculosis, sarcoidosis, syphilis and herpes simplex virus, varicella-zoster virus, rubella virus, and toxoplasmosis genomic DNA in the aqueous samples, as assessed by PCR and immunocompetence. The IOP was determined using a Goldmann tonometer. In all patients, the anterior eye segment and optic disc were examined by glaucoma or uveitis specialists using a slit-lamp biomicroscope and dilated funduscopy to diagnose glaucoma.

AH Collection

AH samples were collected as described previously.³¹ Briefly, in eyes with PSS, AH was collected in the outpatient clinic before commencement of treatment. Under topical anesthesia, approximately 70 to 100 μ L of AH was obtained using a 30-gauge syringe, collected in a ProteoSave SS 1.5-mL Slim-tube (Sumitomo Bakelite, Tokyo, Japan), and then registered and stored at -80°C until processing. For cataract controls, the AH was collected at the beginning of cataract surgery, after paracentesis was performed.

Measurement of Cytokines in the AH

The cytokine levels in the AH were measured using the Bio-Plex Pro Human Cytokine 27-Plex Immunoassay (Bio-Rad Laboratories, Hercules, CA, USA), following the manufacturer's protocols.

Culturing of Human Corneal Endothelial Cells

Primary culturing of human corneal endothelial cells (hCECs) was performed as described previously.³² The cells were cultured at 37°C in 5% CO_2 , and cells from passages 57 to 60 were used for the experiments.

Virus Infection

We used an endotheliotropic human cytomegalovirus (HCMV) strain AD169/rev for hCEC infection. AD169/rev is a virus mutant strain modified from AD169 so that it can easily infect endothelial cells, including ARPE-19, which can be used for a CMV cell line or replication of the virus.³³ To obtain AD 169/rev, the culture fluid from ARPE-19 cells transfected with AD169/rev clone at a multiplicity of infection (MOI) of 0.4 was collected after culturing for 5 days. The culture supernatants were harvested, followed by centrifugation for 10 minutes at 3000 rpm at room temperature to prepare cell-free CMV medium. The harvested medium was used after one cycle of freezing and thawing. After reaching confluence, the hCECs were incubated with the cell-free CMV medium for 2 hours at 37°C in 5% CO_2 with a MOI of 1. After exposure, the cell-free CMV medium was removed, and the infected cells were washed twice with $1\times$ PBS, followed by incubation in growth medium. Infected hCECs were then grown in the growth medium. To confirm whether hCECs were infected, the cells were stained with Mouse Anti-Cytomegalovirus Monoclonal Antibody (MAB810R), clone 8B1.2 (Sigma-Aldrich, St. Louis, MO, USA), which reacts with an immediate-early (IE) non-structural antigen of 68–72 kDa, to check the expression of IE antigen. The IE antigen was detected 1 day after exposure to cell-free CMV medium (Supplementary Figure S1).

Immunocytochemistry

Immunocytochemistry (ICC) was performed as previously described.³⁴ The cells were grown in chamber slides. The hCECs were fixed in ice-cold 4% paraformaldehyde for 15 minutes 1 day after infection and then permeabilized with 0.3% Triton X-100 (Sigma-Aldrich) for 5 minutes and blocked in 3% BSA for 30 minutes. The primary antibodies were anti-CMV, clone 8B1.2 (1:2000; Sigma-Aldrich); anti-ZO-1 (1:100; Abcam, Cambridge, UK); anti-TNF- α (1:500; Abcam); and anti-nuclear factor kappa B (NF- κ B) (1:100; Sigma-Aldrich). Alexa Fluor 488 and 594 secondary antibodies (1:1000) were purchased from Thermo Fisher Scientific (Waltham, MA, USA). We further determined if changes induced by CMV infection were suppressed by ROCK inhibitors (Y27632, K115), because the Rho-ROCK pathway is a common downstream component of TNF- α signaling.

Quantitative PCR

The cells were lysed using TRI Reagent (Molecular Research Center, Inc., Cincinnati, OH, USA), and mRNA was isolated using chloroform and isopropyl alcohol. The mRNA was treated with a PrimeScript RT Reagent Kit (Takara Bio, Shiga, Japan) to synthesize cDNA. mRNA was quantified using quantitative PCR (qPCR) with SYBR Premix Ex Taq II (Tli RNase H Plus) (Takara Bio) and the Thermal Cycler Dice Real Time System II (Takara Bio) using the $\Delta\Delta\text{Ct}$ method. For qPCR, primer sequences were taken from previously published sequences, and the primers were purchased from Hokkaido System Science (Hokkaido, Japan). The sequences of the PCR primers were as follows: glyceraldehyde 3-phosphate dehydrogenase (GAPDH), forward, 5'-GAGTCAACGGATTTGGTGTG-3', and reverse, 5'-TTGATTTTGGAGGGATCTCG-3'; IL-10, forward, 5'-GCCTAACATGCTTCGAGATC, and reverse, 5'-TGATGCTGGGTCTTGGTTC; and TNF- α , forward,

5'- CCCGAGTGACAAGCCTGTAG, and reverse, 5'- GATG-GCAGAGAGGAGGTTGAC. The data were normalized relative to GAPDH.

Cell Fractionation

CMV-infected hCECs with or without ROCK inhibitors (Y27632, K115) or JSH-23 (inhibitor of NF- κ B transcriptional activity) were fractionated using the Abcam Cell Fractionation Kit (Standard) following the manufacturer's protocol.

Western Blotting

One day after CMV infection with or without Y27632 or K115, the cells were collected in RIPA buffer (Thermo Fisher Scientific) containing protease inhibitors (Roche Diagnostics, Basel, Switzerland). They were then sonicated and centrifuged. Western blotting (WB) was performed as described previously.³⁴ The primary antibodies were as follows: anti-TNF- α (1:500; Abcam), anti-NF- κ B (1:100; Sigma-Aldrich), anti-IL-10 (1:500; Abcam), Phospho-I κ B α (Ser32/36) (5A5) antibody (1:1000, Cell Signaling Technology), and anti-GAPDH (1:1000; Wako Pure Chemical Industries, Osaka, Japan). Horseradish peroxidase (HRP)-conjugated secondary antibody (1:2000) was purchased from Thermo Fisher Scientific. The bands were quantified using ImageJ 1.49 software (National Institutes of Health, Bethesda, MD, USA).

Evaluation of Apoptosis and Cell Death

After incubation, we used the Vybrant Apoptosis Assay Kit (Thermo Fisher Scientific) to quantify apoptotic hCECs infected with CMV. After CMV infection, the hCECs were stained using Alexa Fluor 488-conjugated annexin V binding combined with propidium iodide labeling. Apoptotic hCECs were stained as annexin V(+)/propidium iodide(-), and necrotic cells were stained as annexin V(+)/propidium iodide(+). Undamaged hCECs remained negative for both stains.^{35,36} At the end of the double-staining procedure, Hoechst 33342 was added to the culture medium to a final concentration of 8 mM. The cells were counted in at least seven random fields of each well at 200 \times magnification using a fluorescence microscope (BZ-9000; Keyence, Tokyo, Japan). The percentages of apoptotic hCECs and necrotic hCECs were quantified by determining the ratio of annexin V(+)/propidium iodide(-) cells and annexin V(+)/propidium iodide(+) cells to Hoechst 33342(+) retinal ganglion cells, respectively. The cells were counted in a masked manner.

RhoA Activation Assay

RhoA is a Rho GTPase, a family within the Ras superfamily of monomeric small guanosine triphosphate (GTP)-binding proteins that act as molecular switches that cycle between a GTP-bound active and a GDP-bound inactive conformation. We also performed RhoA activation assays to confirm whether CMV infection in hCECs can induce RhoA. Thirty minutes after CMV infection, RhoA activation was examined using a pull-down assay (RhoA Activation Assay Biochem Kit; Cytoskeleton, Inc., Denver, CO, USA), according to the manufacturer's instructions. HRP-conjugated secondary antibody (1:1000) was purchased from Thermo Fisher Scien-

tific. Protein bands were detected using an ImageQuant LAS 4000 mini biomolecular imager (GE Healthcare, Chicago, IL, USA). The bands were quantified using Adobe Photoshop (Adobe Inc., San Jose, CA, USA).

Measurement of Monolayer Cell Permeability and Monolayer Transendothelial Electrical Resistance in the hCECs

To measure the monolayer cell permeability, hCECs were grown on Corning Transwell polycarbonate membrane inserts (0.4- μ m pore size and 12-mm diameter; Sigma-Aldrich) on 12-well culture plates (BD Falcon, Franklin Lakes, NJ, USA) at 37°C in 5% CO₂ until confluent as previously described.³⁷ The volume of the applied medium was 0.5 mL on the apical side (inside of the membrane inserts) and 1.5 mL on the basal side (outside of the membrane inserts). Two weeks after seeding, hCEC-cell monolayers were exposed to the cell-free CMV medium for 2 hours and washed with PBS(-) twice, and we further determined if changes induced by CMV infection were suppressed by ROCK inhibitors (Y27632, K115) or JSH-23. A 4-kDa FITC-dextran dye (Sigma-Aldrich) was simultaneously applied together with those inhibitors at 50 μ M to the basal compartment of the wells. Also, transendothelial electrical resistance (TEER) was recorded using Millicell ERS (Sigma-Aldrich) according to the manufacturer's instructions. The medium was collected from the apical side for fluorescence measurements at 1, 3, 6, and 12 hours after adding the dye, and the same volume of fresh culture medium was replaced. The concentration of FITC-dextran in the collected medium was measured using a multimode plate reader (MTP-800AFC Multi-Detection Microplate Reader; Corona Electric, Ibaragi, Japan), with an excitation wavelength of 490 nm and an emission wavelength of 530 nm. Fluorescence intensity of the normal medium was measured as the background concentration in each experiment. Also, time-dependent changes of TEER were compared as percent change of reduction from baseline values. Each experiment was repeated at least three times.

Statistical Analysis

The data were statistically analyzed using the EZR program (Saitama Medical Center, Hidaka, Japan).³⁸ The results are expressed as mean \pm standard deviation (SD). The *t*-test and χ^2 or Fisher's exact test were used for comparing two variables, and the Steel-Dwass test was used for analyzing multiple variables. Differences among groups were analyzed by one-way ANOVA and Tukey's test as a post hoc test. A value of *P* < 0.05 was considered statistically significant.

RESULTS

Demographic Data of the Study Population

Table 1 lists the demographic data of the study population. There were 20 subjects in the control group (eyes without any ocular complications) and 19 CMV-positive PSS patients. The ratio of males to females was 8:12 in the control group and 15:4 in the CMV+/PSS group (Table 1). The IOP was significantly higher in the CMV+/PSS group compared to the control group (Table 1). The number of corneal endothelial cells was significantly lower in the CMV+/PSS group compared to the control group (Table 1). The

TABLE 1. Demographic Characteristics of the Study Population

Variables	Control	CMV+/PSS	P*
Patients (n)	20	19	—
Eyes (n)	20	19	—
Gender, male:female (n)	8:12	15:4	<0.005 [†]
Age (y), mean ± SD (range)	73.5 ± 3.8 (58–87)	62.7 ± 7.4 (39–86)	<0.005 [‡]
IOP (mm Hg), mean ± SD (range)	13.5 ± 0.7 (12–16)	19.6 ± 4.0 (8–34)	<0.001 [‡]
Corneal endothelial cells (n), mean ± SD (range)	2644.9 ± 123.5 (2321–3251)	2027.1 ± 355.5 (388–2778)	<0.001 [‡]
Glaucoma eye drops (n), mean ± SD (range)	—	0.8 ± 2.1 (0–4)	—
Aqueous TNF-α level (pg/mL), mean ± SD (range)	4.0 ± 9.1 (0–34.71)	45.3 ± 28.8 (3.4–79.5)	<0.0001 [‡]

* All P represent a statistically significant difference between control and CMV+/PSS (Steel-Dwass test).

[†] Fisher's exact test.

[‡] Mann-Whitney U-test.

TABLE 2. Comparing the Concentrations (pg/mL) of Each Cytokine

Variables	Mean ± SD (range)		P*
	Control	CMV+/PSS	
IL-1β	0.05 ± 0.02 (0.02–0.09)	0.23 ± 0.33 (0.22–0.99)	NS
IL-1Ra	93.73 ± 7.81 (6.88–259.4)	193.09 ± 154.54 (43.86–504.39)	NS
IL-8	13.87 ± 13.08 (4.14–61.22)	49.09 ± 29.34 (18.52–116.21)	<0.001
IL-10	0.45 ± 0.37 (0.04–1.19)	10.50 ± 11.86 (0.40–38.15)	<0.001
MCP-1	287.96 ± 124.82 (164.26–647.78)	791.25 ± 1122.7 (227.22–3917.48)	<0.05
Eotaxin	4.95 ± 1.74 (1.95–8.10)	12.37 ± 35.64 (2.52–35.64)	<0.01
FGF	2.00 ± 2.58 (0.07–11.70)	5.06 ± 5.34 (0.07–15.88)	NS
IFN-γ	6.58 ± 4.94 (0.67–20.84)	30.04 ± 50.27 (2.21–161.17)	NS
IL-4	0.12 ± 0.06 (0.08–0.22)	0.72 ± 0.67 (0.08–1.60)	<0.05
IL-6	12.90 ± 18.30 (0.79–74.87)	11.00 ± 13.89 (0.79–35.85)	NS
IL-7	4.33 ± 3.41 (0.78–14.94)	4.16 ± 2.62 (0.78–7.79)	NS
IL-9	1.46 ± 1.25 (0.31–4.02)	4.10 ± 4.72 (0.76–7.44)	NS
IL-12	0.57 ± 0.67 (0.08–3.22)	0.39 ± 0.28 (0.08–0.96)	NS
IL-13	1.42 ± 0.21 (1.27–1.57)	1.85 ± 1.90 (0.5–3.19)	NS
IL-17	1.76 ± 3.49 (0.06–11.05)	5.56 ± 8.35 (0.06–24.93)	NS
RANTES	5.44 ± 0.92 (3.02–6.84)	24.14 ± 41.21 (2.65–139.36)	<0.001

* Mann-Whitney U-test.

aqueous and overall levels of TNF-α were significantly higher in the CMV+/PSS group compared to the control group ($P < 0.001$; Table 1).

The IL-8, IL-10, eotaxin, monocyte chemoattractant protein-1 (MCP-1), IL-4, and RANTES (regulated upon activation, normal T-cell expressed and secreted) levels were significantly higher in the CMV+/PSS group compared to the control group ($P < 0.01$) (Table 2).

The number of corneal endothelial cells was negatively correlated with the aqueous TNF-α level (Spearman's rank correlation coefficient: -0.391 , $P < 0.05$) (Table 1, Fig. 1A), and the aqueous level of IL-10 was negatively correlated with the number of corneal endothelial cells (Fig. 1C). However, there was no significant correlation between the number of corneal endothelial cells and the levels of IL-8, eotaxin, MCP-1, IL-4, or RANTES (Figs. 1B, 1D, 1E, 1F, and 1G, respectively).

Assessment by WB of IL-10 Expression in CMV-Infected hCECs

Figure 2A shows the WB data ($n = 3$), which indicated that the expression of IL-10 was slightly upregulated with CMV infection. The quantitative analysis showed that the expres-

sion of IL-10 was significantly upregulated at 1 day after infection (Fig. 2B).

Activated RhoA

Figure 2C shows the data from the RhoA activation assay ($n = 3$), indicating that the expression of active RhoA was upregulated after CMV infection. The quantitative analysis showed that the expression of active RhoA was significantly upregulated at 1 day after infection (Fig. 2D).

CMV-Induced mRNA Expression of IL-10 and TNF-α

We analyzed the mRNA expression levels of IL-10 and TNF-α in CMV-infected hCECs using qRT-PCR (Figs. 2E, 2F). Basal levels of IL-10 and TNF-α were detectable in CMV-infected hCECs, and, compared with the control, CMV infection significantly increased the expression of IL-10 and TNF-α ($P < 0.001$) (Figs. 2E, 2F). When the ROCK inhibitors (Y27632, K115) or JSH-23 were applied after CMV infection, the expression of TNF-α was significantly downregulated ($P < 0.01$ for Y27632; $P < 0.001$ for K115 and JSH-23) (Fig. 2F).

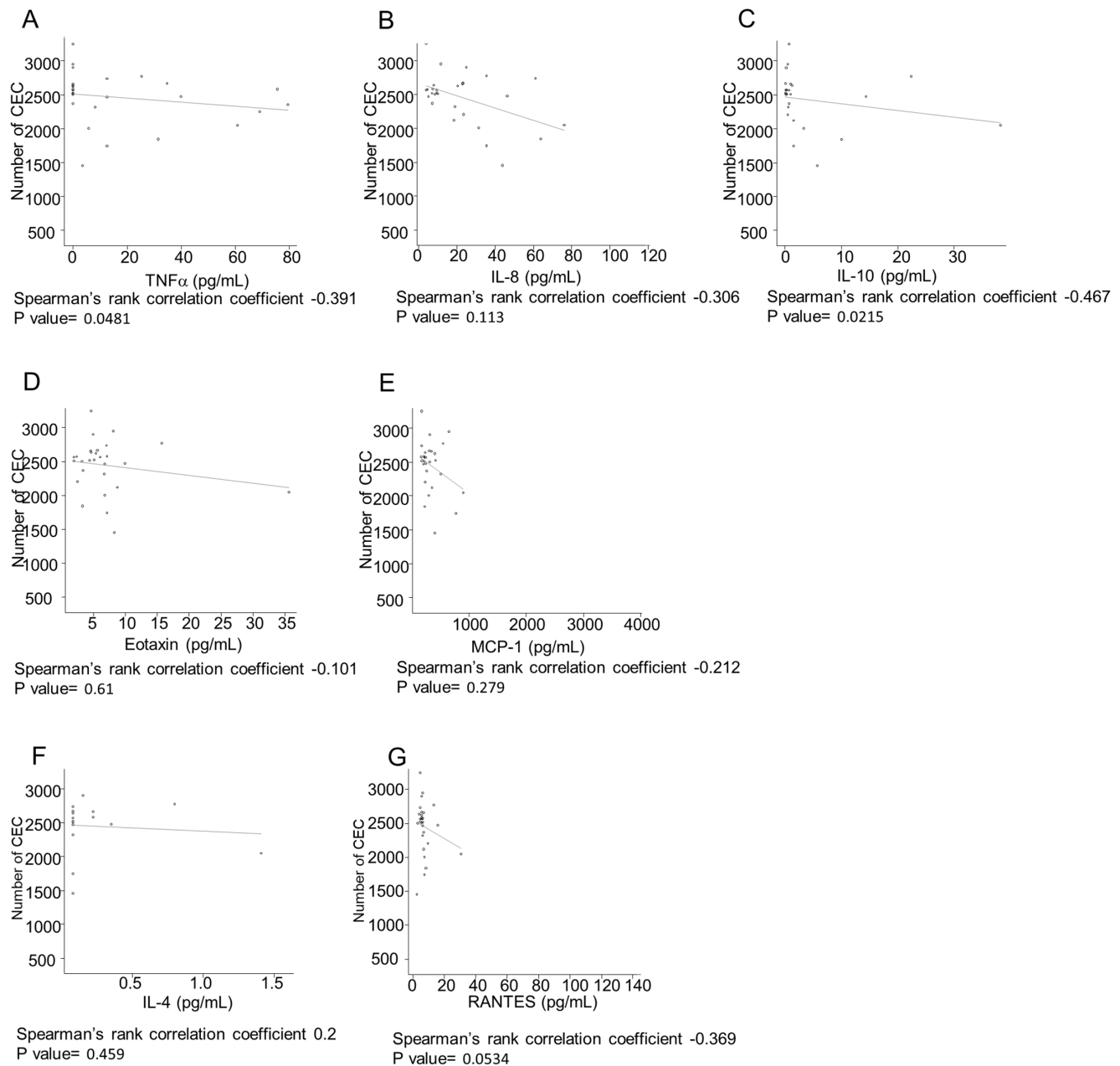


FIGURE 1. Relationship between aqueous cytokine level and the number of corneal endothelial cells in CMV-positive PSS patients, showing aqueous cytokine levels in PSS patients as measured by a multiplex assay. (A, C) The aqueous TNF- α and IL-10 levels were negatively correlated with the number of corneal endothelial cells ($P < 0.05$). (B, D-G) The aqueous IL-10, eotaxin, MCP-1, IL-4, and RANTES levels had no relationship with the number of corneal endothelial cells.

Assessment by ICC and WB of TNF- α , NF- κ B, and Phospho-I κ B α Expression in CMV-Infected hCECs

First, ICC and WB were used to assess the expression levels of TNF- α , NF- κ B, and Phospho-I κ B α after CMV infection. Figure 3 shows the immunocytochemistry results, which indicate that the expression levels of TNF- α and NF- κ B were upregulated after CMV infection but attenuated after treatment with ROCK inhibitors (Fig. 3). Figure 4 shows the WB results ($n = 3$), which also indicate that the expression levels of TNF- α (Fig. 4A), NF- κ B (Fig. 4C) and Phospho-I κ B α (Fig. 4E) were upregulated at 1 day after infection but attenuated after treatment with ROCK inhibitors. Also,

expression of Phospho-I κ B α was downregulated with JSH-23. The quantitative analysis showed that the expression levels of TNF- α , NF- κ B, and Phospho-I κ B α were significantly upregulated at 1 day after infection (Figs. 4B, 4D, 4F).

Effect of CMV Infection on Apoptosis and Necrosis of hCEC

Figure 5 shows representative fluorescence microscopy images of Hoechst 33342 and annexin V/propidium iodide staining at 1 day after infection. The green staining denotes annexin V-positive cells (Fig. 5A), the red

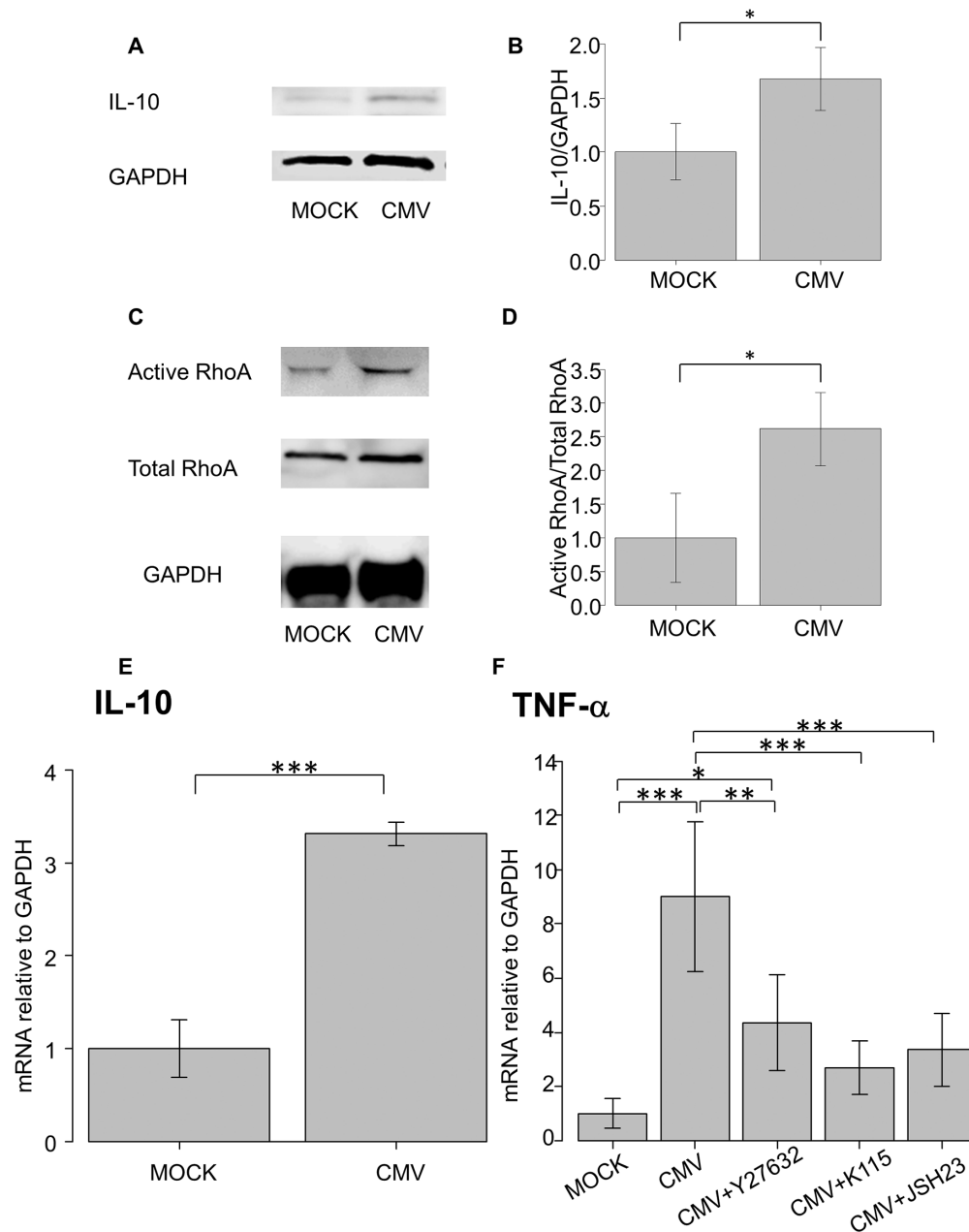


FIGURE 2. (A, B) Western blotting of IL-10 in CMV-infected hCECs. The bands for WB are shown in A, and B shows the relative expression of IL-10 ($n = 3$). The results are expressed relative to the loading control of GAPDH. IL-10 was upregulated in hCECs with CMV infection. $^*P < 0.05$. (C, D) RhoA activation assay of in CMV-infected hCECs. The bands for WB are shown in C, and the expression of active RhoA ($n = 3$) relative to total RhoA is shown in D. Active RhoA was upregulated in hCECs with CMV infection. $^*P < 0.05$. (E, F) qPCR quantification of IL-10 and TNF- α in CMV-infected hCECs. The relative mRNA expression of IL-10 (E) and TNF- α (F) was significantly higher in CMV-infected cells compared to the control. When the ROCK inhibitors (Y27632, K115) or JSH-23 were applied after CMV infection, the expression of TNF- α was significantly downregulated. RT-qPCR with GAPDH primers was performed to serve as an internal control for input DNA. Data are the averages of four independent DNA samples from the infected cells. Values are the mean \pm SE. $^*P < 0.05$, $^{**}P < 0.01$, $^{***}P < 0.001$.

staining denotes propidium iodide-positive cells (Fig. 5B), and the blue staining denotes Hoechst 33342-positive cells (Fig. 5C). Figure 5D is a merged image showing annexin V(+)/propidium iodide(-) apoptotic cells (white arrow) and annexin V(+)/propidium iodide(+) necrotic cells (yellow arrow). Compared to the normal controls, CMV infection significantly increased apoptosis ($2.4 \pm 1.9\%$ vs. $6.4 \pm 2.0\%$; $P < 0.001$, Wilcoxon rank-sum test) (Fig. 5E)

but not necrosis ($5.0 \pm 1.8\%$ vs. $6.0 \pm 2.6\%$; $P = 0.81$, Wilcoxon rank-sum test) (Fig. 5F). The percentages of apoptotic and necrotic hCECs in the ROCK inhibitor group were $3.8 \pm 0.8\%$ and $7.3 \pm 1.2\%$, respectively, for the Y27632 group ($n = 6$) and $2.6 \pm 1.2\%$ and $4.1 \pm 1.9\%$, respectively, for the K115 group ($n = 6$). Treatment with ROCK inhibitors significantly reduced apoptosis of hCEC.

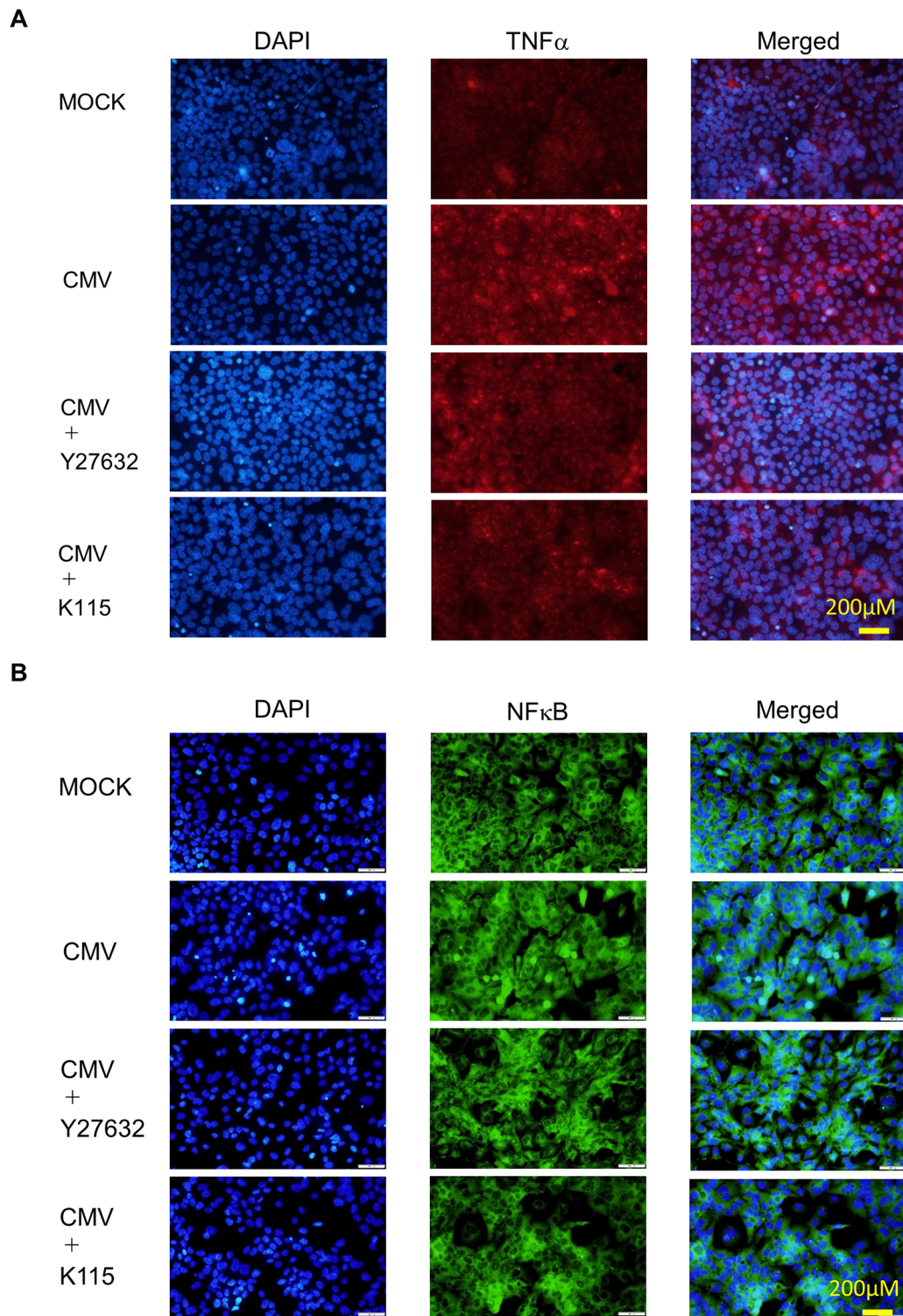


FIGURE 3. ICC of TNF- α and NF- κ B in CMV-infected hCECs. The *left panels* show cells that were stained with 4',6-diamidino-2-phenylindole (DAPI). The *middle panels* show cells stained for TNF- α (**A**) or NF- κ B (**B**). The *right panels* show merged images. The expression data for mock infection are shown in the first row; those for CMV infection, in the second row; those for CMV infection under Y27632, in the third row; and those for CMV infection under K115, in the fourth row. Both TNF- α and NF- κ B expression levels were higher after infection but were attenuated in the presence of ROCK inhibitors. *Scale bar:* 200 μ m.

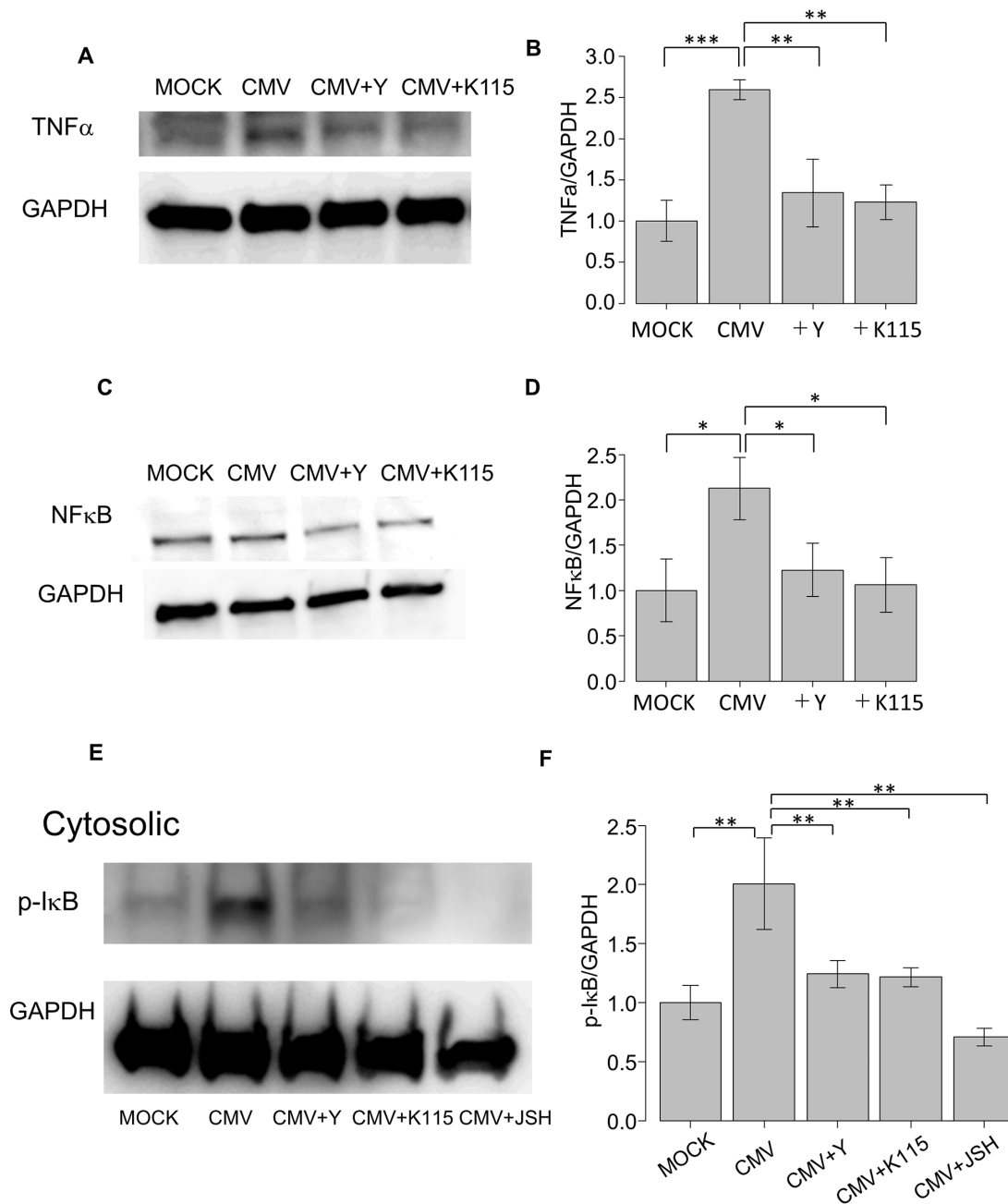


FIGURE 4. WB of TNF- α , NF- κ B, and Phospho-I κ B α in CMV-infected hCECs showing the expression levels of TNF- α (A), NF- κ B (C), and Phospho-I κ B α (E). In the *left row*, the bands for WB are shown; in the *right row*, the expression levels of TNF- α , NF- κ B, and Phospho-I κ B α ($n = 3$) and the results expressed relative to the loading control (GAPDH) are shown. (B, D, F) These components were upregulated in hCECs with CMV infection and downregulated in the presence of ROCK inhibitors. Also, the expression of and Phospho-I κ B α was downregulated with JSH-23. * $P < 0.05$; ** $P < 0.01$; *** $P < 0.001$.

Cell-Cell Contact and Cell Permeability in hCECs Assessed by FITC-Dextran Flux and TEER

In an attempt to confirm the effect of ROCK inhibitors to restore the decreased cell-cell adhesion and barrier function in CMV-infected hCECs, we performed permeability assays using a flux of FITC-dextran and measurement of TEER in hCECs. CMV infection significantly increased the concentration of FITC-dextran in the apical side of CEC (corneal endothelial cells) cells at 1 and 3 hour after FITC-dextran

exposure ($P < 0.001$ for 1 hour, $P < 0.05$ for 3 hours) (Fig. 6A). Additionally, when ROCK inhibitors (Y27632 and K115) were applied together, those inhibitors significantly attenuated the changes induced by CMV infection 1 hour after FITC-dextran exposure ($P < 0.01$) (Fig. 6A). Also, Y27632 significantly attenuated the changes induced by CMV infection at 3 hours after FITC-dextran exposure; K115 failed to show significance ($P = 0.096$). There was no significant difference at 6 and 12 hours after FITC-dextran exposure. Although JSH-23 failed to show significant differences

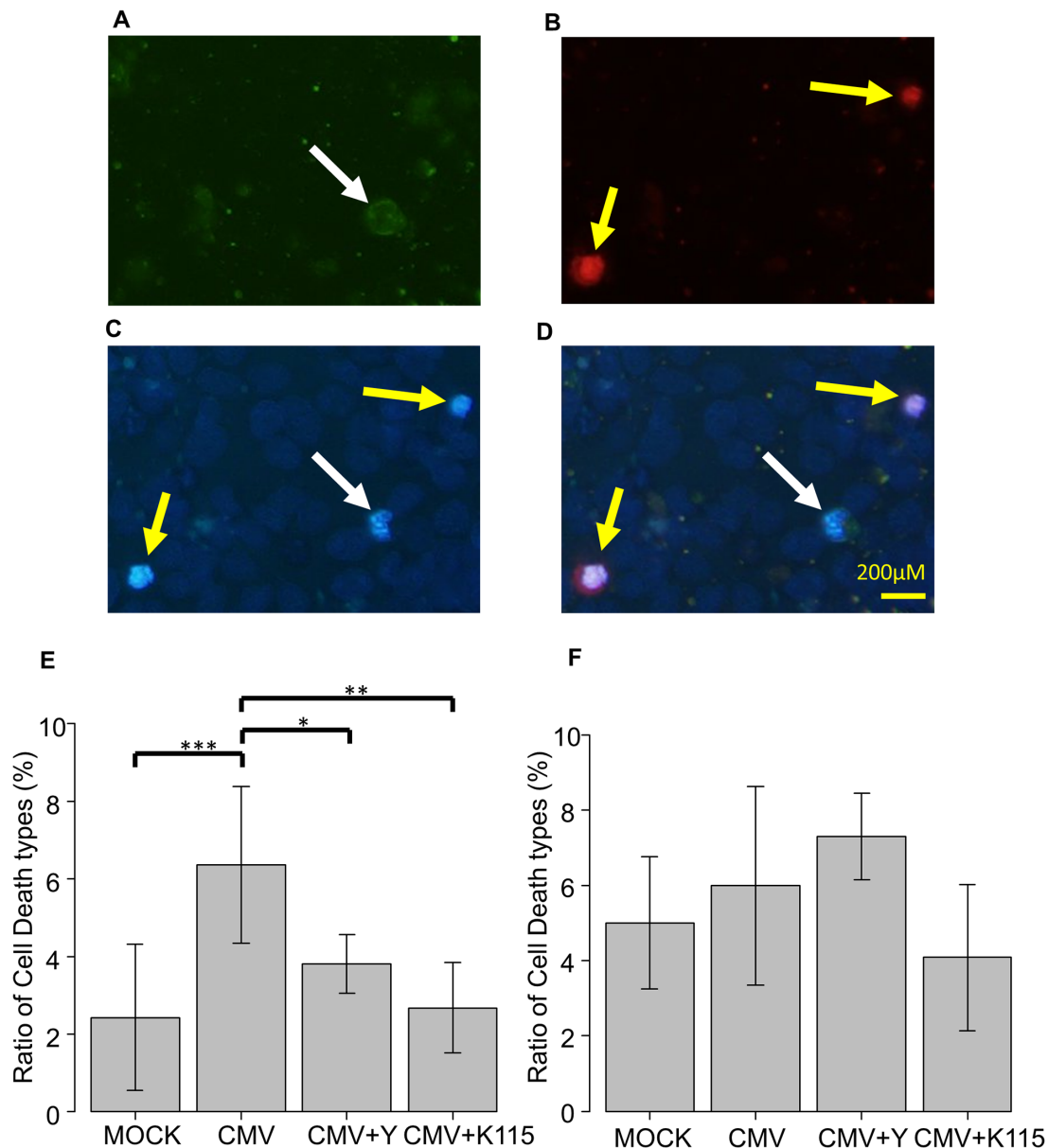


FIGURE 5. Representative fluorescence microscopy images of Hoechst 33342 and annexin V/propidium iodide staining at 24 hours after CMV infection to detect apoptotic and necrotic hCECs post-CMV infection with or without ROCK inhibitors. (A) *Green staining* is annexin V-positive cells. (B) *Red staining* is propidium iodide-positive staining cells. (C) *Blue staining* is Hoechst 33342-positive staining cells. (D) Merged image showing annexin V(+)/propidium iodide(-) apoptotic cells (*white arrow*) and annexin V(+)/propidium iodide(+) necrotic cells (*yellow arrow*). (E) Ratio of apoptotic cells. CMV infection increased the percentage of apoptotic cells, and ROCK inhibitors significantly decreased the CMV infection-induced expression of apoptotic cells. (F) The expression level of necrotic cells did not differ among groups. Each value represents the mean \pm SD ($n = 6$). * $P < 0.05$; ** $P < 0.01$; *** $P < 0.001$.

among mock infections at any time points, it did show a tendency to suppress the increased TEER at 1 hour and 3 hours ($P = 0.062$ and $P = 0.066$, respectively).

Figure 6B shows the results of the TEER on CMV infection and whether or not those changes were attenuated with ROCK inhibitors (Y27632, K115) or JSH-23. CMV infection showed significant decrease in TEER at 3, 6, and 12 hours after CMV infection, and the change in TEER was significantly restored when ROCK inhibitors (Y27632, K115) or JSH-23 were applied. These observations suggested that simultaneous administration of ROCK inhibitors

(Y27632, K115) or JSH-23 inhibited the CMV infection-induced a decrease in the barrier functions of the hCEC monolayer.

Barrier Integrity and Cytoskeletal Changes in hCEC as Assessed by ICC

The expression of zonula occludens-1 (ZO-1) and F-actin was decreased in CMV-infected hCECs compared to the control group (Figs. 7A, 7B), and these CMV

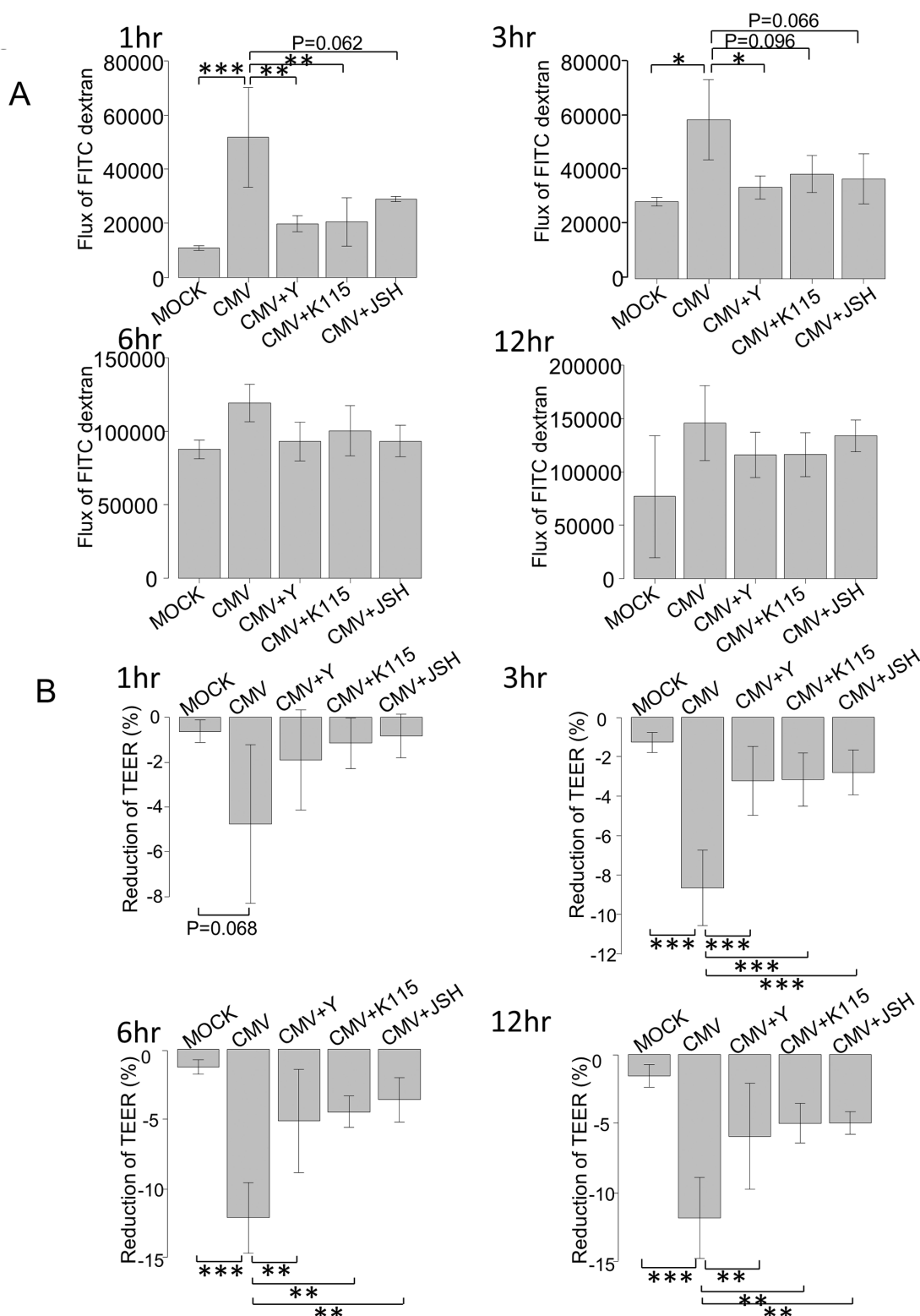


FIGURE 6. Measurement of monolayer cell permeability in CMV-infected hCECs with or without inhibitors. **(A)** Changes in the hCEC monolayer permeability using 4-kDa FITC-dextran are shown. hCECs were infected with CMV, and concentrations were measured at 1, 3, 6, and 12 hours after exposure of the FITC-dextran. Mean values from four separate filters are presented. hCEC monolayer permeability was significantly increased after CMV infection at 1 hour and 3 hours. hCEC monolayer permeability decreased in the presence of the ROCK inhibitors (Y27632, 100 μ M; K115, 100 μ M). Although JSH-23 (10 μ M) failed to show a significant difference, it did show a tendency to suppress the increased TEER at 1 hour and 3 hours ($P = 0.062$ and $P = 0.066$, respectively). $*P < 0.05$, $**P < 0.01$, $***P < 0.001$. **(B)** Effect of CMV infection on TEER in hCEC monolayer. hCECs were infected with CMV. TEER was measured at 1, 3, 6, and 12 hours from infection. Data are shown as mean values \pm SE from four separate filters. TEER in the hCEC monolayer was significantly reduced after CMV infection at 3, 6, and 12 hours. The decrease in TEER was attenuated with the presence of the ROCK inhibitors (Y27632, 100 μ M; K115, 100 μ M) or JSH-23 (10 μ M). $**P < 0.01$, $***P < 0.001$.

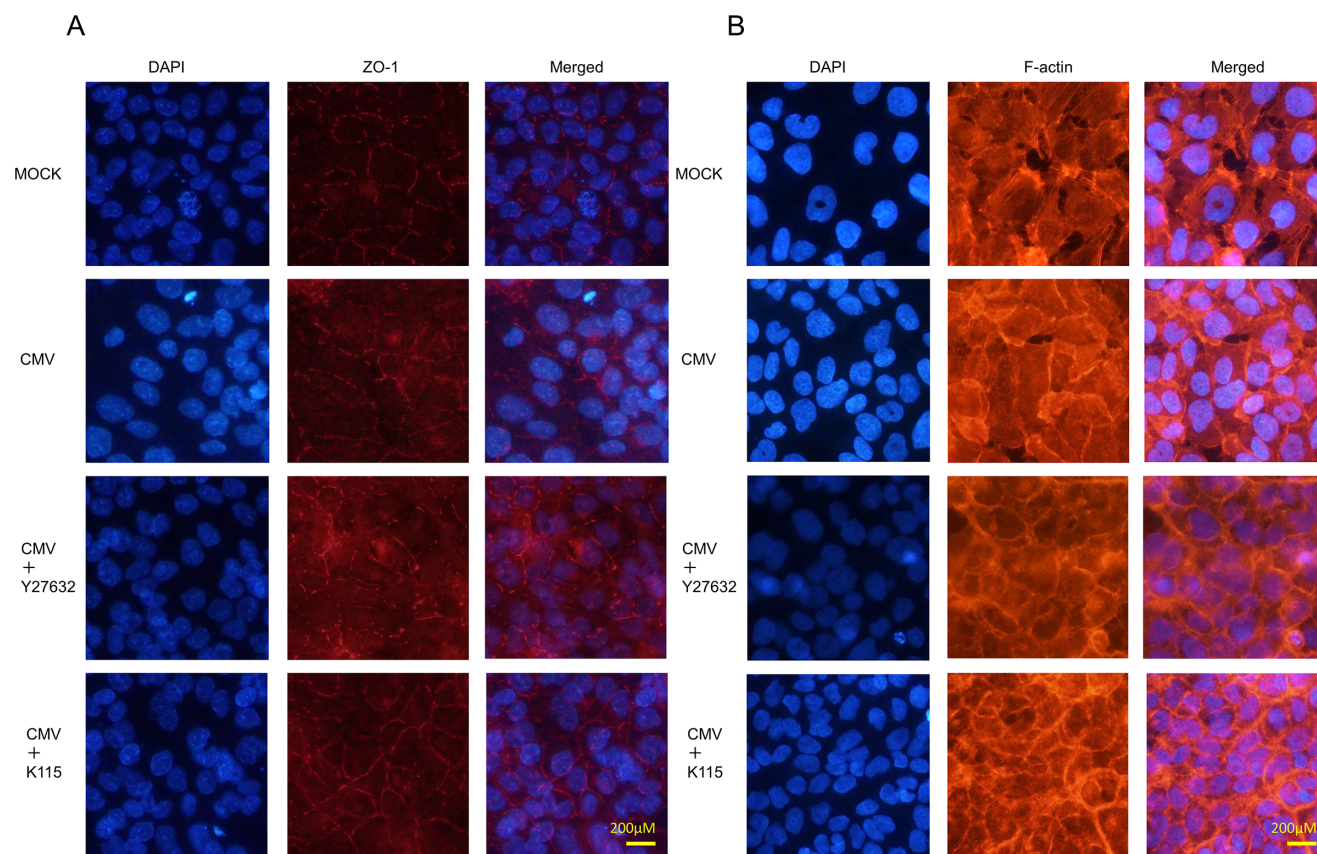


FIGURE 7. ICC of ZO-1 and F-actin in hCECs infected with CMV. **(A)** The *left panels* show cells that were stained with DAPI, the *middle panels* show cells stained for ZO-1, and the *right panels* show merged images. The expression data for mock infection are shown in the first row; those for CMV infection, in the second row; those for CMV infection in the presence of Y27632, in the third row; and those for CMV infection in the presence of K115, in the fourth row. Cell–cell contact was impaired after CMV infection, but this change was attenuated by ROCK inhibitors. *Scale bar:* 200 μm . **(B)** The *left panels* show cells that were stained with DAPI, the *middle panels* show cells stained for F-actin, and the *right panels* show merged images. The expression data for mock infection are shown in the first row; those for CMV infection, in the second row; those for CMV infection under Y27632, in the third row; and those for CMV infection in the presence of K115, in the fourth row. Cytoskeletal formation was impaired after CMV infection, but this change was attenuated by ROCK inhibitors. *Scale bar:* 200 μm .

infection-induced changes were significantly attenuated in the presence of ROCK inhibitors (Y27632, K115).

DISCUSSION

In this study, we found that the concentration of TNF- α in aqueous samples of CMV-positive PSS patients was significantly higher compared to healthy control patients without ocular inflammatory conditions, and the aqueous TNF- α negatively correlated with the number of corneal endothelial cells. Several studies have reported changes in the aqueous cytokine profiles of different clinical entities of uveitis, including infectious uveitis,³⁹ Bechet's disease, Vogt–Koyanagi–Harada disease,^{40,41} Fuchs' heterochromic cyclitis (FHC), and other types of clinically idiopathic uveitis.^{42–45} Increased levels of IL-6, MCP-1, and IL-8 are commonly observed in ocular inflammatory diseases, and similar changes in these cytokines have also been reported in PSS patients.⁷ It has been reported that PSS patients show a stronger and more active ocular inflammatory response compared to healthy controls and FHC patients, with higher concentrations of IL-1RA, IL-8, and IL-10.^{7,10} In the present study, we also found that the IL-8, IL-10, eotaxin, MCP-1,

IL-4, and RANTES levels were significantly higher in the CMV+/PSS group compared to the control group ($P < 0.01$) (Table 2), and the elevations in levels of MCP-1, IL-8, and IL-10 were consistent with previous reports. Among the upregulated cytokines, there was no significant correlation between the number of corneal endothelial cells and levels of IL-8, eotaxin, MCP-1, IL-4, or RANTES (Figs. 1B, 1D, 1E, 1F, and 1G, respectively), but TNF- α and IL-10 (Figs. 1A and 1C, respectively) showed significant correlations with decreased corneal endothelial cells.

However, there were some discrepancies among previous reports regarding the aqueous levels of TNF- α in PSS patients. Li et al.⁷ evaluated the differences in aqueous cytokine levels between PSS patients with and without CMV, but they failed to detect aqueous TNF- α in PSS patients, regardless of the presence of CMV viral DNA. However, a recent study by Pohlmann et al.¹⁰ reported that the aqueous TNF- α level was significantly higher compared to the control. In the present study, we found significantly higher levels of TNF- α in CMV+/PSS patients compared to controls, which is consistent with the latter report.

Because we found that TNF- α and IL-10 levels were upregulated in CMV+/PSS patients and showed significant

correlations with the decrease in corneal endothelial cells (Tables 1 and 2 and Figs. 1A and 1C, respectively), we conducted in vitro studies to confirm whether the TNF- α and IL-10 levels were induced by CMV infection in hCECs. First, we used ICC to confirm CMV infection in hCECs (Supplementary Figure S1) and found that infection was established 1 day after infection when the hCECs were exposed to CMV at a MOI of 0.1. Figures 2F, 3A, and 4A show that CMV infection in hCECs was significantly induced by TNF- α expression, which was confirmed by rPCR, ICC, and WB. CMV infection also slightly induced the expression of IL-10 (Figs. 2A, 2B, 2E). CMV+/PSS is known to cause chronic uveitis with a higher recurrence rate; in such incidents, due to the chronic inflammatory state, antiinflammatory cytokines including IL-10 may be induced to antagonize the uveitis. Barton et al.^{46,47} reported that in animal models of experimental autoimmune uveitis, the T cells found in the early stage of the disease were mainly CD4+T cells secreting Th1-type cytokines (IFN- γ) and that in the latter stage a shift was taking place toward the Th2 type cytokines (IL-10). Therefore, we hypothesized that chronic inflammatory state in CMV+/PSS may have induced upregulation of IL-10 in the aqueous humor in the present study. Figures 2C and 2D show that using the Rho pull-down assay, CMV-infected hCECs exhibited significant upregulation of active RhoA compared to mock infection. In addition, Figure 3B shows that the translocation of NF- κ B to the nucleus was accelerated after CMV infection, suggesting that TNF- α -related cellular responses, including prolonged inflammation or apoptosis, may be promoted through the upregulation of NF- κ B and RhoA.

TNF- α has been implicated in endothelial dysfunction and apoptosis during corneal allograft rejection and AU.^{11,48,49} Past studies have reported a correlation between TNF- α and ROCK; TNF- α induced activated Rho, whereas ROCK promoted translocation of NF- κ B to the nucleus to accelerate the production of TNF- α .^{50,51} Based on these results, we speculated that higher expression of TNF- α induced CMV-infected hCECs and active RhoA, resulting in translocation of NF- κ B to the nucleus to induce apoptosis. Also, NF- κ B translocation to the nucleus may accelerate the production of TNF- α to maintain RhoA in an activated state.

In the present study, therefore, we focused on TNF- α -Rho-ROCK signaling induced by CMV infection in hCECs, and further characterized the role of TNF- α in corneal endothelial cell death to determine if corneal endothelial cell death was suppressed in the presence of ROCK inhibitors. It has been suggested that Rho-ROCK signaling not only acts on the downstream cascade of TNF- α but also works as a generator of TNF- α . In corneal endothelial cells, it has been reported that overexpression of ROCK1 may trigger lipopolysaccharide-induced production of TNF- α and its downstream apoptosis, which could be attenuated with ROCK inhibitors.⁵¹ Yang et al.⁵⁰ reported a preservative effect of ROCK inhibitors on the apoptosis of microvascular endothelial cells via inhibition of the nuclear translocation of NF- κ B and consequent suppression of the generation of TNF- α . We therefore hypothesize that ROCK inhibitors may modulate the CMV-infection-induced generation of TNF- α . As shown in Figures 2F, 3 and 4, CMV-infection-induced upregulation of TNF- α , NF- κ B, and Phospho-I κ B α was significantly downregulated by ROCK inhibitors (Y27632, K115). Also, the expression of Phospho-I κ B α was downregulated under JSH-23. These data suggest that CMV induces the phosphorylation of I κ B, which leads to

the translocation of NF- κ B into the nucleus to induce apoptosis.

In the next step, we further investigated whether corneal endothelial cells underwent apoptosis post-CMV infection, which would be attenuated by ROCK inhibitors.^{13,20,52,53} We conducted an apoptosis activity assay to confirm whether CMV induced apoptosis in hCECs and whether this was attenuated by ROCK inhibitors. Figure 5 shows that the apoptosis rate was significantly elevated in hCECs during post-CMV infection (Fig. 5E), and these changes were significantly decreased by treatment with ROCK inhibitors. Past reports have shown that endothelial cells infected with CMV rapidly induce apoptosis to oppose viral growth,²⁶ and our results are consistent with this finding. In addition, because ROCK inhibitors are known to alter cell adhesion properties and upregulate cell-cell contacts,⁵⁴ to clarify if ROCK inhibitors (Y27632, K115) can attenuate the changes induced by CMV infection in cell-cell contact and the barrier function, we infected monolayer hCECs and looked for changes in cell permeability.

hCEC permeability increased immediately after CMV infection (Figs. 6A, 6B). This increased permeability was attenuated by ROCK inhibitors (Y27632, K115) and NF- κ B inhibitor (Figs. 6A, 6B). This suggests that CMV induced decreased cell-cell contact and that barrier function can be restored with ROCK inhibition or transcriptional inhibition of NF- κ B (Figs. 6A, 6B). Also, hCECs were stained with ZO-1 after CMV infection. Figures 7A and 7B show that CMV infection significantly impaired cell-cell adhesion, and treatment with ROCK inhibitors significantly restored diminished cell-cell adhesion and cytoskeletal formation. Collectively, ROCK inhibitors showed the potential to protect CMV-infected cells from apoptosis and to maintain cellular integrity.

PSS is characterized by acute and recurrent IOP elevation in unilateral eyes, often accompanied by significant corneal endothelial cell loss; our findings support the hypotheses that dysfunction in hCECs induced by CMV infection can promote TNF- α and its downstream cascade and can trigger severe corneal endothelial cell loss. When the number of corneal endothelial cells has decreased, the condition is irreversible and cannot be treated medically. It has been reported that TNF- α is important in the reactivation of CMV infection.⁵⁵⁻⁵⁷ Figure 4 shows that ROCK inhibitors had the potential to alter TNF- α upregulation induced by CMV infection. Thus, ROCK inhibitors could assist in the treatment of corneal endothelial cell loss of CMV-positive PSS patients.

Our study had several limitations. First, although we typically collected the AH at the time of IOP elevation, we could not compare the levels of TNF- α with that at other times or according to the CMV copy number or CMV infection activity. Further investigation will be needed, including prospective studies, to make these comparisons. Second, the number of AH samples was relatively small, so further studies with larger samples will be necessary to analyze the relationship between the number of corneal endothelial cells and cytokine profiles, for example. Third, the ratio of male subjects to female subjects differed in the control and patient groups in this study. It would be ethically difficult to obtain aqueous humor from healthy young subjects without any ocular diseases who are of the same generation as those affected by PSS, and the number of patients undergoing cataract surgery in their same generation was limited. Fourth, AD169/rev is a virus mutant made from AD169 designed to be tropic for endothelial cells, so the virus strain could be stronger than the clinical virus strains collected in

the patients' aqueous humor. Though the virulence of the CMV strain in this study may deviate from clinical practice because the infectivity depends on cell types, the aqueous cytokine profile changes, and the decreased number of corneal endothelial cells found in CMV-positive PSS patients corresponds to the results of our in vitro study. For this reason, we suggest that our findings on TNF- α upregulation and apoptotic changes in hCECs mimic clinical changes induced with CMV infection. Fifth, this is a retrospective and in vitro study; thus, further experiments using animal models will be needed to explore whether CMV infection in the anterior chamber may induce TNF- α upregulation or corneal endothelial cell loss in the future. Finally, though we preliminarily compared the number of the corneal endothelial cells between control and CMV-/PSS groups, there was no significant difference between those groups (data not shown), and there should be a study that includes CMV-/PSS patients in the future.

In the present study, we found that TNF- α was upregulated in the AH and in CMV-infected hCECs, which may trigger apoptotic changes in hCECs. Modulation of TNF- α and its downstream cascade could therefore serve as a novel and effective treatment for patients with CMV-positive PSS.

Acknowledgments

A statistician reviewed and proofread the statistical analyses in this document, and the language in this document was reviewed by at least two professional editors, both native speakers of English.

The authors thank Naoki Inoue, Professor of Laboratory of Microbiology and Immunology, Gifu Pharmaceutical University, for assistance in obtaining the CMV AD169/rev strain.

Supported by a Grant from the Japan Society for the Promotion of Science (19K09965 to MH), who had designed this research.

Disclosure: **N. Igarashi**, None; **M. Honjo**, None; **T. Kaburaki**, None; **M. Aihara**, None

References

1. Posner A, Schlossman A. Syndrome of unilateral recurrent attacks of glaucoma with cyclitic symptoms. *Arch Ophthalmol*. 1948;39:517–535.
2. Chee SP, Jap A. Presumed Fuchs heterochromic iridocyclitis and Posner-Schlossman syndrome: comparison of cytomegalovirus-positive and negative eyes. *Am J Ophthalmol*. 2008;146:883–889.
3. Chee SP, Bacsal K, Jap A, Se-Thoe S-Y, Cheng CL, Tan BH. Corneal endotheliitis associated with evidence of cytomegalovirus infection. *Ophthalmology*. 2007;114:798–803.
4. Chee SP, Bacsal K, Jap A, Se-Thoe S-Y, Cheng CL, Tan BH. Clinical features of cytomegalovirus anterior uveitis in immunocompetent patients. *Am J Ophthalmol*. 2008;145:834–840.
5. Kandori M, Miyazaki D, Yakura K, et al. Relationship between the number of cytomegalovirus in anterior chamber and severity of anterior segment inflammation. *Jpn J Ophthalmol*. 2013;57:497–502.
6. Hedayatfar A, Chee SP. Posner-Schlossman syndrome associated with cytomegalovirus infection: a case series from a non-endemic area. *Int Ophthalmol*. 2014;34:1123–1129.
7. Li J, Ang M, Cheung CM, et al. Aqueous cytokine changes associated with Posner-Schlossman syndrome with and without human cytomegalovirus. *PLoS One*. 2012;7:e44453.
8. Teoh SB, Thean L, Koay E. Cytomegalovirus in aetiology of Posner-Schlossman syndrome: evidence from quantitative polymerase chain reaction. *Eye (Lond)*. 2005;19:1338–1340.
9. Neri P, Zucchi M, Allegri P, Lettieri M, Mariotti C, Giovannini A. Adalimumab (Humira™): a promising monoclonal anti-tumor necrosis factor alpha in ophthalmology. *Int Ophthalmol*. 2011;31(2):165–173.
10. Pohlmann D, Schlickeiser S, Metzner S, Lenglinger M, Winterhalter S, Pleyer U. Different composition of intraocular immune mediators in Posner-Schlossman Syndrome and Fuchs' Uveitis. *PLoS One*. 2018;13:e0199301.
11. Lindstedt EW, Baarsma GS, Kuijpers RW, van Hagen PM. Anti-TNF-alpha therapy for sight threatening uveitis. *Br J Ophthalmol*. 2005;89:533–536.
12. Lahdou I, Engler C, Mehrle S, et al. Role of human corneal endothelial cells in T-cell-mediated alloimmune attack in vitro. *Invest Ophthalmol Vis Sci*. 2014;55:1213–1221.
13. Srinivas SP. Cell signaling in regulation of the barrier integrity of the corneal endothelium. *Exp Eye Res*. 2012;95:8–15.
14. Shivanna M, Rajashekhar G, Srinivas SP. Barrier dysfunction of the corneal endothelium in response to TNF-alpha: role of p38 MAP kinase. *Invest Ophthalmol Vis Sci*. 2010;51(3):1575–1582.
15. Hu J, Zhang Z, Xie H, Chen L, et al. Serine protease inhibitor A3K protects rabbit corneal endothelium from barrier function disruption induced by TNF- α . *Invest Ophthalmol Vis Sci*. 2013;54:5400–5407.
16. Goldblum SE, Ding X, Campbell-Washington J. TNF-alpha induces endothelial cell F-actin depolymerization, new actin synthesis, and barrier dysfunction. *Am J Physiol*. 1993;264:C894–905.
17. Petrache I, Birukova A, Ramirez SI, Garcia JG, Verin AD. The role of the microtubules in tumor necrosis factor-alpha-induced endothelial cell permeability. *Am J Respir Cell Mol Biol*. 2003;28(5):574–581.
18. Okada N, Fukagawa K, Takano Y, et al. The implications of the upregulation of ICAM-1/VCAM-1 expression of corneal fibroblasts on the pathogenesis of allergic keratopathy. *Invest Ophthalmol Vis Sci*. 2005;46:4512–4518.
19. Watsky MA, Guan Z, Ragsdale DN. Effect of tumor necrosis factor alpha on rabbit corneal endothelial permeability. *Invest Ophthalmol Vis Sci*. 1996;37:1924–1929.
20. McKenzie JA, Ridley AJ. Roles of Rho/ROCK and MLCK in TNF-alpha-induced changes in endothelial morphology and permeability. *J Cell Physiol*. 2007;213:221–228.
21. Petrache I, Crow MT, Neuss M, Garcia JG. Central involvement of Rho family GTPases in TNF-alpha-mediated bovine pulmonary endothelial cell apoptosis. *Biochem Biophys Res Commun*. 2003;306:244–249.
22. Shivanna M, Srinivas SP. Elevated cAMP opposes (TNF-alpha)-induced loss in the barrier integrity of corneal endothelium. *Mol Vis*. 2010;16:1781–1790.
23. Wang Q, Wei C, Ma L, et al. Inflammatory cytokine TNF- α promotes corneal endothelium apoptosis via upregulating TIPE2 transcription during corneal graft rejection. *Graefes Arch Clin Exp Ophthalmol*. 2018;256:709–715.
24. Rajashekhar G, Shivanna M, Kompella UB, Wang Y, Srinivas SP. Role of MMP-9 in the breakdown of barrier integrity of the corneal endothelium in response to TNF- α . *Exp Eye Res*. 2014;122:77–85.
25. Hosogai M, Shima N, Nakatani Y, et al. Analysis of human cytomegalovirus replication in primary cultured human corneal endothelial cells. *Br J Ophthalmol*. 2015;99:1583–1590.

26. Brune W, Ménard C, Heesemann J, Koszinowski UH. A ribonucleotide reductase homolog of cytomegalovirus and endothelial cell tropism. *Science*. 2001;291:303–305.
27. Sabio G, Davis RJ. TNF and MAP kinase signalling pathways. *Semin Immunol*. 2014;26:237–245.
28. Wojciak-Stothard B, Ridley AJ. Rho GTPases and the regulation of endothelial permeability. *Vascul Pharmacol*. 2002;39:187–199.
29. Mathew SJ, Haubert D, Krönke M, Leptin M. Looking beyond death: a morphogenetic role for the TNF signalling pathway. *J Cell Sci*. 2009;122:1939–1946.
30. Jabs DA, Nussenblatt RB, Rosenbaum JT, Standardization of Uveitis Nomenclature (SUN) Working Group. Standardization of uveitis nomenclature for reporting clinical data. Results of the First International Workshop. *Am J Ophthalmol*. 2005;140:509–516.
31. Honjo M, Igarashi N, Kurano M, et al. Autotaxin-lysophosphatidic acid pathway in intraocular pressure regulation and glaucoma subtypes. *Invest Ophthalmol Vis Sci*. 2018;59:693–701.
32. Shima N, Kimoto M, Yamaguchi M, Yamagami S. Increased proliferation and replicative lifespan of isolated human corneal endothelial cells with L-ascorbic acid 2-phosphate. *Invest Ophthalmol Vis Sci*. 2011;52:8711–8717.
33. Kobayashi R, Abe M, Oguri K, et al. Analysis of relationships between polymorphisms in the genes encoding the pentameric complex and neutralization of clinical cytomegalovirus isolates. *Vaccine*. 2018;36:5983–5989.
34. Igarashi N, Honjo M, Kurano M, et al. Increased aqueous autotaxin and lysophosphatidic acid levels are potential prognostic factors after trabeculectomy in different types of glaucoma. *Sci Rep*. 2018;8:11304.
35. Schutte B, Nuydens R, Geerts H, Ramaekers F. Annexin V binding assay as a tool to measure apoptosis in differentiated neuronal cells. *J Neurosci Methods*. 1998;86:63–69.
36. Tezel G, Yang X. Caspase-independent component of retinal ganglion cell death, in vitro. *Invest Ophthalmol Vis Sci*. 2004;45:4049–4059.
37. Kaneko Y, Ohta M, Inoue T, et al. Effects of K-115 (Ripasudil), a novel ROCK inhibitor, on trabecular meshwork and Schlemm's canal endothelial cells. *Sci Rep*. 2016;6:19640.
38. Kanda Y. Investigation of the freely available easy-to-use software 'EZ' for medical statistics. *Bone Marrow Transplant*. 2013;48:452–458.
39. Takase H, Futagami Y, Yoshida T, et al. Cytokine profile in aqueous humor and sera of patients with infectious or noninfectious uveitis. *Invest Ophthalmol Vis Sci*. 2006;47:1557–1561.
40. Ahn JK, Yu HG, Chung H, Park YG. Intraocular cytokine environment in active Behçet uveitis. *Am J Ophthalmol*. 2006;142:429–434.
41. El-Asrar AM, Struyf S, Kangave D, et al. Cytokine profiles in aqueous humor of patients with different clinical entities of endogenous uveitis. *Clin Immunol*. 2011;139:177–184.
42. Calder VL, Shaer B, Muhaya M, et al. Increased CD4+ expression and decreased IL-10 in the anterior chamber in idiopathic uveitis. *Invest Ophthalmol Vis Sci*. 1999;40:2019–2024.
43. Curnow SJ, Falciani F, Durrani OM, et al. Multiplex bead immunoassay analysis of aqueous humor reveals distinct cytokine profiles in uveitis. *Invest Ophthalmol Vis Sci*. 2005;46:4251–4259.
44. Lacomba MS, Martin CM, Chamond RR, Galera JM, Omar M, Estevez EC. Aqueous and serum interferon gamma, interleukin (IL) 2, IL-4, and IL-10 in patients with uveitis. *Arch Ophthalmol*. 2000;118:768–772.
45. Ooi KG, Galatowicz G, Towler HM, Lightman SL, Calder VL. Multiplex cytokine detection versus ELISA for aqueous humor: IL-5, IL-10, and IFN-gamma profiles in uveitis. *Invest Ophthalmol Vis Sci*. 2006;47:272–277.
46. Barton K, Lightman S. T lymphocyte effector mechanisms in the retina in posterior uveitis. *Eye (Lond)*. 1994;8:60–65.
47. Barton K, McLauchlan MT, Calder VL, Lightman S. The kinetics of cytokine mRNA expression in the retina during experimental autoimmune uveoretinitis. *Cell Immunol*. 1995;164:133–140.
48. Niederkorn JY, Mayhew E, Mellon J, Hegde S. Role of tumor necrosis factor receptor expression in anterior chamber-associated immune deviation (ACAID) and corneal allograft survival. *Invest Ophthalmol Vis Sci*. 2004;45:2674–2681.
49. Wang Q, Wei C, Ma L, et al. Inflammatory cytokine TNF- α promotes corneal endothelium apoptosis via upregulating TIPE2 transcription during corneal graft rejection. *Graefes Arch Clin Exp Ophthalmol*. 2018;256:709–715.
50. Yang J, Ruan F, Zheng Z. Ripasudil attenuates lipopolysaccharide (LPS)-mediated apoptosis and inflammation in pulmonary microvascular endothelial cells via ROCK2/eNOS signaling. *Med Sci Monit*. 2018;24:3212–3219.
51. Gong J, Guan L, Tian P, Li C, Zhang Y. Rho kinase type 1 (ROCK1) promotes lipopolysaccharide-induced inflammation in corneal epithelial cells by activating Toll-like receptor 4 (TLR4)-mediated signaling. *Med Sci Monit*. 2018;24:3514–3523.
52. Eisa-Beygi S, Wen XY. Could pharmacological curtailment of the RhoA/Rho-kinase pathway reverse the endothelial barrier dysfunction associated with Ebola virus infection? *Antiviral Res*. 2015;114:53–56.
53. Yang L, Tang L, Dai F, et al. Raf-1/CK2 and RhoA/ROCK signaling promote TNF- α -mediated endothelial apoptosis via regulating vimentin cytoskeleton. *Toxicology*. 2017;389:74–84.
54. Okumura N, Koizumi N, Ueno M, et al. ROCK inhibitor converts corneal endothelial cells into a phenotype capable of regenerating in vivo endothelial tissue. *Am J Pathol*. 2012;181:268–277.
55. Simon CO, Seckert CK, Dreis D, Reddehase MJ, Grzimek NK. Role for tumor necrosis factor alpha in murine cytomegalovirus transcriptional reactivation in latently infected lungs. *J Virol*. 2005;79:326–340.
56. Cook CH, Trgovcich J, Zimmerman PD, Zhang Y, Sedmak DD. Lipopolysaccharide, tumor necrosis factor alpha, or interleukin-1beta triggers reactivation of latent cytomegalovirus in immunocompetent mice. *J Virol*. 2006;80:9151–9158.
57. Döcke WD, Prösch S, Fietze E, et al. Cytomegalovirus reactivation and tumour necrosis factor. *Lancet*. 1994;343:268–269.